INFORMATION TO USERS

This dissertation was produced from a microfilm copy of the original document. While the most advanced technological means to photograph and reproduce this document have been used, the quality is heavily dependent upon the quality of the original submitted.

The following explanation of techniques is provided to help you understand markings or patterns which may appear on this reproduction.

1. The sign or "target" for pages apparently lacking from the document photographed is "Missing Page(s)". If it was possible to obtain the missing page(s) or section, they are spliced into the film along with adjacent pages. This may have necessitated cutting thru an image and duplicating adjacent pages to insure you complete continuity.

2. When an image on the film is obliterated with a large round black mark, it is an indication that the photographer suspected that the copy may have moved during exposure and thus cause a blurred image. You will find a good image of the page in the adjacent frame.

3. When a map, drawing or chart, etc., was part of the material being photographed the photographer followed a definite method in "sectioning" the material. It is customary to begin photoing at the upper left hand corner of a large sheet and to continue photoing from left to right in equal sections with a small overlap. If necessary, sectioning is continued again — beginning below the first row and continuing on until complete.

4. The majority of users indicate that the textual content is of greatest value, however, a somewhat higher quality reproduction could be made from "photographs" if essential to the understanding of the dissertation. Silver prints of "photographs" may be ordered at additional charge by writing the Order Department, giving the catalog number, title, author and specific pages you wish reproduced.

University Microfilms

300 North Zeeb Road
Ann Arbor, Michigan 48106

A Xerox Education Company

A SEARCH FOR FRACTIONALLY CHARGED PARTICLES IN COSMIC RAYS AT MOUNTAIN ALTITUDE

by

Aaron J. Cox, Jr.

A Dissertation Submitted to the Faculty of the

DEPARTMENT OF PHYSICS

In Partial Fulfillment of the Requirements
For the Degree of

DOCTOR OF PHILOSOPHY

In the Graduate College

THE UNIVERSITY OF ARIZONA

1 9 7 1

THE UNIVERSITY OF ARIZONA

GRADUATE COLLEGE

I hereby recommend that this dissertation prepared under my direction by Aaron J. Cox Jr.

entitled A Search for Fractionally Charged Particles in Cosmic Rays at Mountain Altitude

be accepted as fulfilling the dissertation requirement of the degree of Doctor of Philosophy

Theodore Bowen — Dissertation Director

11/19/70 — Date

After inspection of the final copy of the dissertation, the following members of the Final Examination Committee concur in its approval and recommend its acceptance:*

L.C. McIntyre	Nov 19, 1970
W. E. Conway	Nov 19, 1970
J. M. Cushing	Nov. 20, 1970
R. L. Thews	Nov. 20, 1970

*This approval and acceptance is contingent on the candidate's adequate performance and defense of this dissertation at the final oral examination. The inclusion of this sheet bound into the library copy of the dissertation is evidence of satisfactory performance at the final examination.

STATEMENT BY AUTHOR

This dissertation has been submitted in partial fulfillment of requirements for an advanced degree at The University of Arizona and is deposited in the University Library to be made available to borrowers under rules of the Library.

Brief quotations from this dissertation are allowable without special permission, provided that accurate acknowledgment of source is made. Requests for permission for extended quotation from or reproduction of this manuscript in whole or in part may be granted by the head of the major department or the Dean of the Graduate College when in his judgment the proposed use of the material is in the interests of scholarship. In all other instances, however, permission must be obtained from the author.

SIGNED: Aaron J. Cox Jr.

ACKNOWLEDGMENTS

I am indebted to those who inspired, advised, and assisted me in all phases of this experiment. I first wish to thank Mr. W. T. Beauchamp, my co-worker on the project, whose assistance and collaboration was invaluable. I would also like to thank Dr. T. Bowen for his inspiration and guidance during all phases of the experiment; Dr. R. M. Kalbach and Dr. A. Pifer for many helpful discussions; Dr. E. P. Krider for much help and advice during his operation of a previous similar experiment; Mr. J. O. Evans and Mr. G. R. Sitz for their help with the construction of equipment; Mr. J. O. Evans, Mr. T. L. Charlton, and Mr. H. B. Barber for their help in obtaining the data; Miss L. S. Graves, Miss R. J. Ferry, and Mr. A. P. Pitucco for their help with the data analysis.

TABLE OF CONTENTS

LIST OF ILLUSTRATIONS

LIST OF TABLES

ABSTRACT

A scintillation counter telescope consisting of eight liquid scintillation counters and four wide gap spark chambers was used to search for particles with electric charge ±1/3e and ±2/3e in cosmic rays at 9000 feet above sea level. No such particles were detected during the 1500 hour experimental run, establishing upper limits on the vertical fluxes of these particles of 8.3×10^{-11} cm^{-2} sec^{-1} sr^{-1} for charge ±1/3e and 9.6×10^{-11} cm^{-2} sec^{-1} sr^{-1} for charge ±2/3e at a 90% confidence level.

INTRODUCTION

The quark model was proposed, independently, by Gell-Mann (1) and Zwieg (2) in 1964. It is based on three, as yet, mathematical objects called quarks. These objects are hypothetically treated as particles and assigned quantum numbers for charge, baryon number, spin, isospin and strangeness. Table I summarizes their properties. Combinations of quarks are used to theoretically construct or generate the irreducible SU(3) groups of baryons and mesons. For example, the proton and neutron are considered as a grouping of three quarks, while the π meson would be a quark-anti-quark pair. Table II shows the $(1/2)^+$ baryon octet and the $(0)^-$ meson octet as they would be constructed from the quark and anti-quark triplets.

Since 1964, the quark model has enjoyed considerable success as a theoretical basis for calculating the properties of certain strongly interacting particles. Scattering cross sections (3), decay rates (4), magnetic moments (5), and mass splittings within multiplets (6) have all been treated with varying success using the quark model. Each success of the model as a mathematical tool has encouraged those who choose to consider quarks as physical objects. Indeed, this possibility has occupied

Table I Quantum Numbers of Quarks

Quark Symbol	Charge Q	Isospin		Strangeness	Baryon Number	Spin
		I	I_z			
p	$+\frac{2}{3}$	$\frac{1}{2}$	$+\frac{1}{2}$	0	$\frac{1}{3}$	$\frac{1}{2}$
n	$-\frac{1}{3}$	$\frac{1}{2}$	$-\frac{1}{2}$	0	$\frac{1}{3}$	$\frac{1}{2}$
λ	$-\frac{1}{3}$	0	0	-1	$\frac{1}{3}$	$\frac{1}{2}$

Table II Quark Content of Meson (0^-) Octet and Baryon ($1/2^+$) Octet

Pseudoscalar Mesons ($J^P = 0^-$)

Particle	Quark Content	Ispin	Strangeness
π^+	$p\bar{n}$	1	0
π^0	$\frac{1}{\sqrt{2}}(p\bar{p}-n\bar{n})$	1	0
π^-	$\bar{p}n$	1	0
K^0	$n\bar{\lambda}$	1/2	1
K^+	$p\bar{\lambda}$	1/2	1
$\bar{K}_0$	$n\lambda$	1/2	-1
K^-	$\bar{P}\lambda$	1/2	-1
S	$\frac{1}{\sqrt{6}}(\bar{p}p+\bar{n}n-2\bar{\lambda}\lambda)$	0	0

Low Lying Baryon Octet ($J^P = 1/2^+$)

Particle	Quark Content	Ispin	Strangeness
p	ppn	1/2	0
n	pnn	1/2	0
Σ^+	$pp\lambda$	1	-1
Λ	$pn\lambda^*$	0	-1
Σ^-	$nn\lambda$	1	-1
Σ^0	$pn\lambda^*$	1	-1
Ξ^0	$p\lambda\lambda$	1/2	-2
Ξ^-	$n\lambda\lambda$	1/2	-2

*a suitable linear combination of these quarks

experimentalists since the model was first proposed. Several experimental techniques have been employed in search of physical quarks.

The most direct methods involve attempts to produce free quarks in high energy proton-nucleon interactions. Particle accelerators have been used in experiments at Brookhaven (7), CERN (8), SLAC (9), and Serpukhov (10). None of these experiments has detected free quarks. The negative results of these experiments may be due to the limited available energy, a maximum of 70 GeV. To extend the search to higher energy interactions a more energetic particle source is needed.

Primary cosmic radiation is such a source, with incident proton energies above 10^{14} eV, while the atmosphere itself provides the target nuclei. A single ultra-high energy proton-nucleon interaction produces as many as 10^{5} secondary particles called a cosmic ray shower. Free quarks may be among these shower particles. Several techniques are used to search for the quark component of cosmic ray showers.

One method supposes that quarks are very massive particles. Such particles could be produced with velocities considerably less than c, yet carry large kinetic energy and would be preceded by the highly relativistic particles making up the bulk of the shower. The technique

is to trigger detectors upon arrival of a shower, then look for an energetic local shower due to the interaction of the delayed massive quark a short time later. A typical delay time would be of the order of 30 nsec (11).

A second method is to directly search for massive, energetic cosmic ray particles using either a mass spectrometer with time of flight counters (12) or Cerenkov counters and an absorber-counter array to measure residual range (13).

A third type of experiment and the subject of this paper looks for the low ionization energy loss of relativistic fractionally charged particles in dE/dx counters (14) (15). The abundant flux of muons serves to characterize the energy loss for unit charged particles to which the smaller quark energy losses are compared. If quark velocities are non-relativistic this method is ineffective since the energy loss curve, dE/dx, for charged particles rises sharply as velocities drop below minimum ionizing values, but most quarks would be expected to be relativistic if they are produced in high energy collisions.

None of the previous experiments have produced convincing evidence for the physical existence of quarks. Their results establish upper limits on the quark flux in cosmic rays usually stated at the 90% confidence level. The lowest results are of the order of 10^{-10} cm^{-2} sec^{-1} sr^{-1}.

Cairns, McCusker, Peak, and Woolcott have reported observing quark-like tracks in their Wilson cloud chamber experiment (16) (17). They believe the tracks were produced by 2/3e quarks in cosmic ray shower cores. This conclusion is put into serious question by other authors who have shown that the number of tracks observed is consistent with that expected from statistical fluctuations of drop formation and relativistic variations of dE/dx (18) (19) (20). Chu, Kim, Beam, and Kwak have reported obtaining a high energy cosmic ray bubble chamber picture containing a single quark-like track (21). However, lack of experimental data on the bubble growth rate in their chamber casts considerable doubt on their conclusion (22). The results of these groups establish a possible quark flux at sea level of about 5×10^{-10} cm^{-2} sec^{-1} sr^{-1}. This is about five times higher than the lowest upper limits obtained by other investigators. These cloud chamber and bubble chamber results await further analysis and experimental verification, but appear to fall short of confirming the quark's physical existence.

Some authors have expressed the possibility that quarks may be rather light particles; perhaps with masses of about 400 MeV/c, or roughly one third of a nucleon mass (23) (24) (25). Their low production cross section at accelerator energies might then be explained in terms of a very large repulsive barrier in the quark-quark potential.

Typical strong interactions have four momentum transfers of about 0.5 $(GeV/c)^2$. Light quarks, strongly interacting with nuclei in the atmosphere, could easily be slowed to non-relativistic velocities. If this were true, or if for any other reason free quarks were highly attenuated in the atmosphere, cosmic ray quark searches at sea level might be unfavorable for detecting free quarks.

Since most of the previous cosmic ray quark searches were done at sea level, a mountain altitude quark search was undertaken. A large cosmic ray telescope was installed and operated at The University of Arizona's high altitude (9,000 ft.) cosmic ray laboratory near Tucson. The experimental results are the subject of this paper.

APPARATUS

The experimental apparatus was designed to detect single relativistic, fractionally charged particles that might be present in cosmic radiation. It consisted of a stack of eight scintillation counters and four wide gap spark chambers. Since the characteristic energy loss, dE/dx, for a charged particle passing through matter is proportional to the square of its charge, fractionally charged particles would be conspicuous due to their low energy loss in a detector. A typical minimum ionizing ± 1/3e or ± 2/3e charged particle, passing through a detector, would lose 1/9 or 4/9 as much energy as a minimum ionizing unit charged particle. Since the energy loss is subject to statistical fluctuations, the low energy loss must be coincidently observed in several counters to minimize the number of background events. Noise in the electronics, soft showers, and gamma rays also contribute to the number of background events which is minimized by this multi-counter coincidence technique. To further lower the background, four wide gap spark chambers were sandwiched between the scintillation counters.

The scintillator array consisted of eight liquid scintillation counters stacked vertically at 14-inch

intervals. Pairs of wide gap spark chambers were placed between counters 3 and 4 and counters 5 and 6 (Fig. 1). The total height of the array from the top of counter number 1 to the bottom of counter number 8 was 13 ft. Each counter consisted of an 84 in. x 72 in. x 6 in. UVT Plexiglas tray divided into three compartments by fluid-tight Plexiglas walls (Fig. 2). The center compartment was 72 in. x 72 in. and was filled to a depth of 5 inches with a scintillator and mineral oil solution manufactured by Pilot Chemical Inc. The outer compartments were 72 in. x 12 in. and were filled to a depth of 5 inches with pure mineral oil. Three 5-inch EMI-9618B photomultiplier (P.M.) tubes were optically coupled to the outside of the 72 in. walls of the outer compartments (26). This provided a total of six P.M. tubes viewing the scintillator light through the intermediate mineral oil compartments which served as light guides. The light guides kept the signal variation with particle path position in the scintillator to less than 10%. Alternate counters were rotated by 90^{o} about a vertical axis to insure against a particle passing through the guides and producing a coincidence signal due to Cerenkov radiation.

The positive signals from the last dynode of each tube were passively mixed, as were the negative anode signals. This resulted in a single positive and negative signal from each of the eight counters for a single event. The pulse height resolution of each counter was about 33%

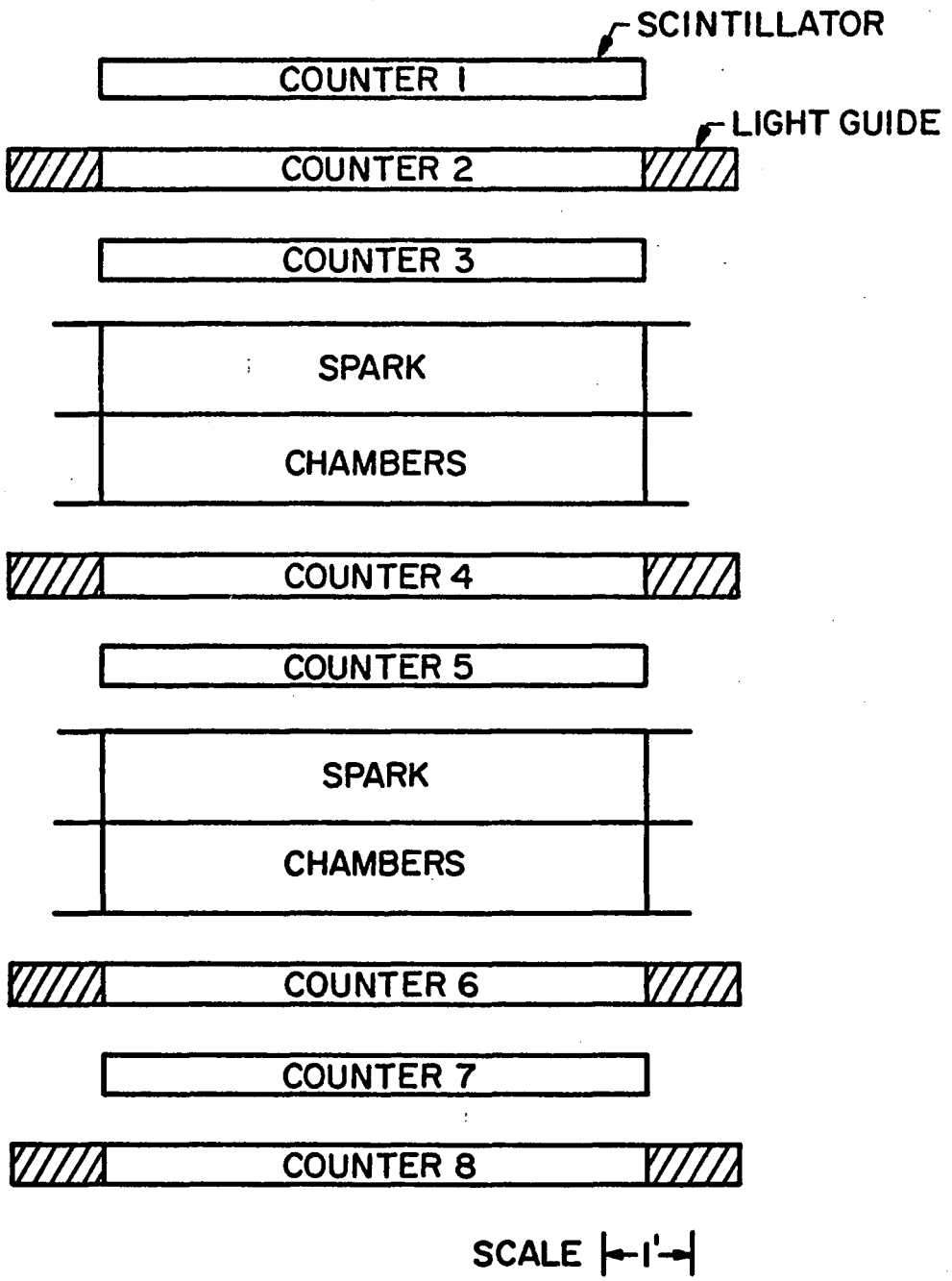

Figure 1 Scintillation counter and spark chamber array. (Crosshatching shows alternated light guides.)

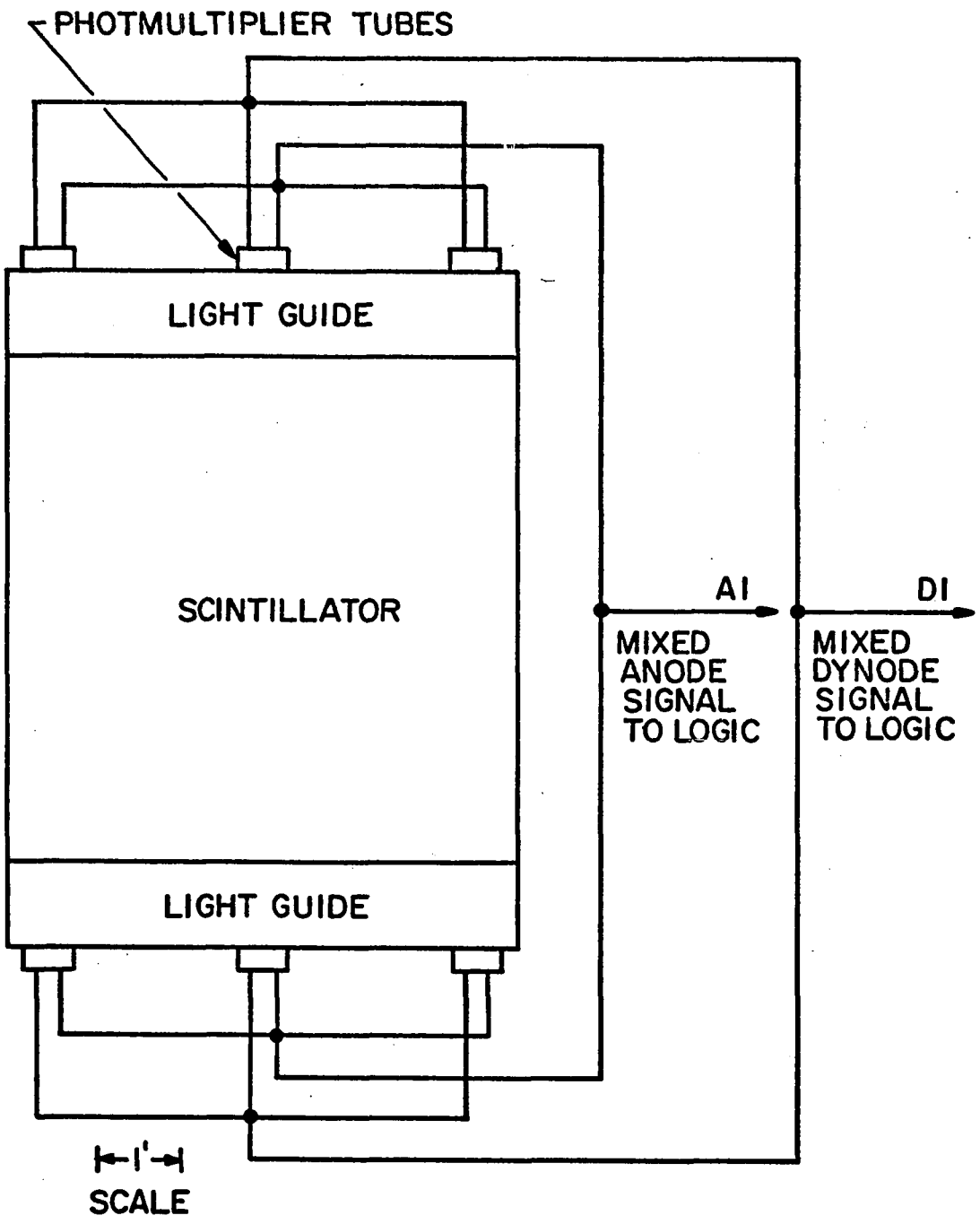

Figure 2 Top view of scintillation counter number 1. (Shown are divided compartments, photomultiplier tubes, and signal mixing scheme used.)

full width at half maximum on unit charged particles. Theoretically calculated pulse height distributions had 20% full widths at half maximum due to Symon-Landau fluctuations only.

The spark chambers insured that a coincidence event in the scintillation counters was actually produced by the passage of a charged particle through the array. The spark chambers consisted of gastight Plexiglas boxes measuring 72 in. x 72 in. x 12 in., and were stacked in two vertical pairs giving a total thickness of each pair of 2 feet. The chambers were filled with a mixture of 90% He and 10% Ar at atmospheric pressure. Aluminum sheets, 72 in. x 72 in., served as electrodes above, below, and between the chambers of a given pair. The electrodes above and below were held at ground potential, while the electrode between the chambers was connected to the output of an eight stage Marx generator. Each stage was charged to a potential of 26 KV resulting in an output of roughly 208 KV. The total capacitance of each Marx generator was 1560 pf.

A typical event would be accompanied by a spark track in each of the four spark chambers. This would give an observable track roughly 4 feet in total length. These tracks were photographed at an optical distance of 120 ft. by a pulsed double-frame 35mm camera through a 300mm f:5 lens and were recorded on Kodak 2475 film. Angled mirrors

were placed behind the chambers to provide a stereo view of the sparks.

Following an eight fold coincidence which satisfied the pulse height criteria for a ± 1/3e or ± 2/3e charged particle, the spark chambers were pulsed and photographed. A delay of 2 μsec. was inserted before the pulsing to allow the completion of all sensitive electronic operations. This insured that the rf noise from the chambers would not affect the logic. The track-forming efficiency of the spark chambers was about 93% on unit charged particles. Tests were done to simulate the track-forming efficiency for fractionally charged particles (15), and no loss of efficiency was observed.

The array was located at an altitude of 9,000 feet above sea level. There was 750 gm/cm^2 of atmosphere above the site; for comparison, the total thickness of the atmosphere down to sea level is 1033 gm/cm^2. The array itself contained 120 gm/cm^2 of material. The integrated area-solid angle of acceptance of the array was .626 m^2sr. This is a geometric quantity neglecting any possible weighting due to atmospheric attenuation which will be discussed later.

The electronics were divided into two parts as seen in Figure 3. The eight negative anode signals were examined by the fast logic circuits to isolate the characteristic quark-like pulses from the numerous unit charged particle

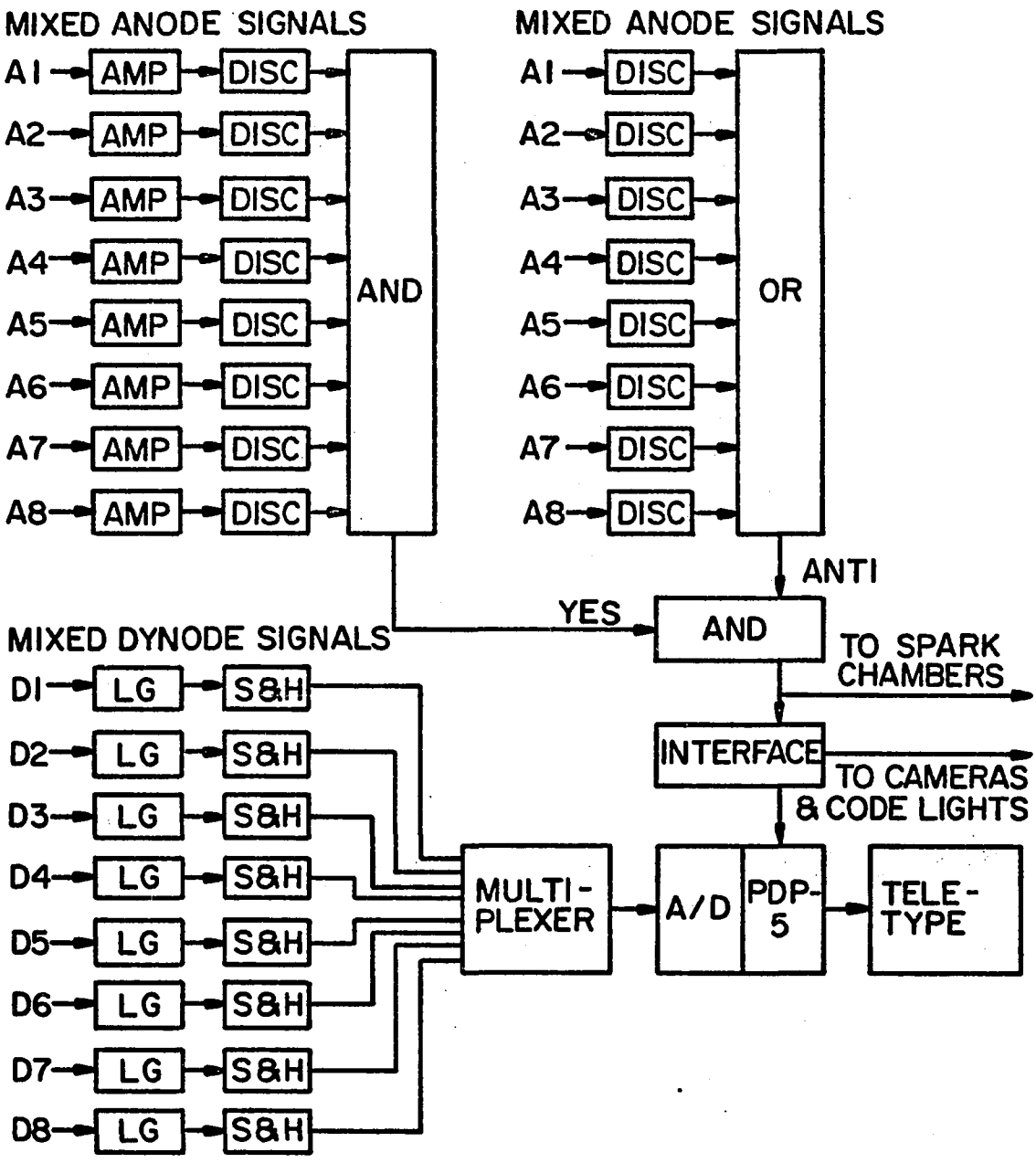

Figure 3 Block diagram of electronics. (AMP. represents an amplifier, DISC a discriminator, LG a linear gate and pulse stretcher, S&H a sample-and-hold circuit, and A/D an analogue to digital converter.)

events. Roughly 100 unit charged particle events were examined each second. An acceptable quark-like event consisted of eight coincident signals each having a pulse height, I, in the range $0.042I_o < I < 0.76I_o$ where I_o is the most probable pulse height of a minimum ionizing unit charged particle. The resolving time of the system was about 15 nsec.

The efficiency of this logic "window" for accepting 1/9 I_o and 4/9 I_o pulses was checked regularly by placing light attenuating screens in front of each photomultiplier tube. These screens consisted of opaque plastic sheets which entirely covered the face of each tube, and in which uniformly spaced holes were drilled so that 1/9 or 4/9 of the surface was removed. Thus the intensity of the light reaching the tubes from the numerous unit charged particle events was reduced to that expected for ± 1/3e or ± 2/3e quarks, and the fluctuations also closely corresponded to those expected for quark events (27). The efficiency of response to these simulated quark events was 93% for the ± 1/3e quarks and 80% for the ± 2/3e quarks. Figure 4 shows the pulse height distribution of charge 1 events as well as those resulting from the simulated ± 1/3e and ± 2/3e quarks.

The positive dynode signals were stored in delay cables while the anode signals were being examined by the fast logic. Whenever an eightfold coincidence satisfied the pulse height requirements, a sequence of operations was

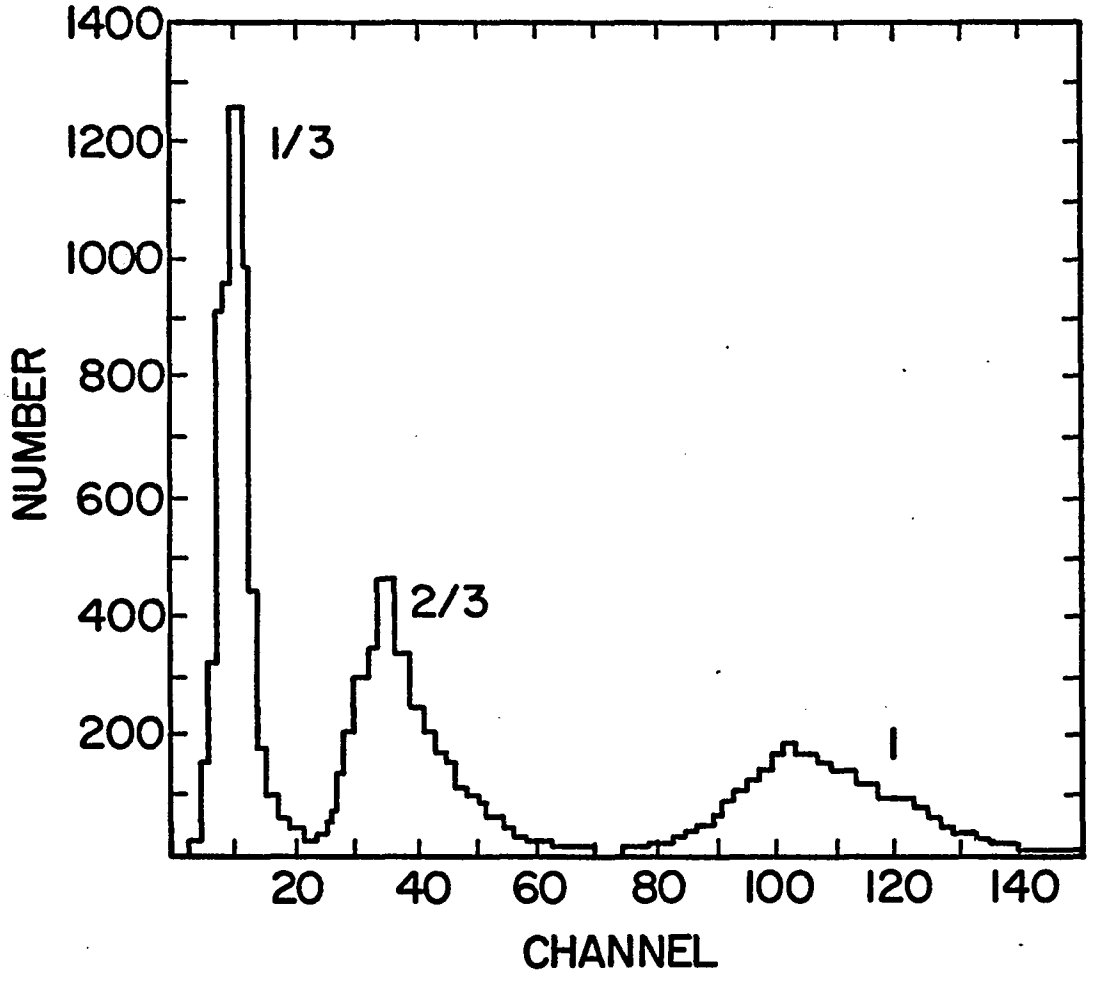

Figure 4 Pulse height distribution of simulated 1/3 and 2/3 quarks and unit charged particles (Each channel equals 12.2 mV)

initiated. First, linear gates and pulse stretcher circuits were opened to permit the dynode signals to be received and stretched in time. The stretched signals were then amplified by a factor of five and held in sample-and-hold circuits. A computer interface circuit generated a set of numbers which uniquely identified this event for later analysis. The signals were then multiplexed into an on-line PDP-5 computer's analogue to digital converter and stored in the computer core memory for analysis.

The eight dynode signals were also sequentially delayed, displayed on an oscilloscope and photographed. These pictures served as a check on the computer output.

Next the spark chambers were pulsed and photographed together with a set of coded lights, which were controlled by the computer interface. They served to correlate the spark chamber pictures with the computer output and oscilloscope pictures. The latter contained an unambiguous duplicate of the coded light pattern received through 20 foot "fiber-optics" light guides.

After each event trigger the electronics were gated off for 2 sec. to allow time for the Marx generators to be recharged. After each event which coincidently satisfied the minimum pulse height requirement ($0.042I_0 < I$) on all eight counters, the electronics were gated off for 200 μsec. This was done to insure against the possibility of photographing the residual spark chamber track left by the

passage of a unit charged particle preceding an event trigger.

The on-line computer analysis consisted of calculating the average pulse height of counters 2 through 7, the r.m.s. deviation of these pulse heights and a parameter, R, given by

$$R = \left(\left(\sum_{i=2}^{7} (P_i - \bar{P}_n)^2\right)/n\right)^{\frac{1}{2}} / \bar{P}_n$$

where P_i is the pulse height of the i^{th} counter and $\bar{P}_n$ is the average pulse height of the six counters. Only six of the eight counters were included in the on-line computer analysis due to computer problems at the time of the run. The parameter, R, was found to be useful in eliminating background events if only events with R < 40% were recorded on the computer output. To be sure that most quark events would have R values less than 40% and would therefore be recorded, the attenuating masks were used to simulate quark-like events and determine the fraction of events that would have values of R less than various percentages. Figure 5 shows the results of these tests. For the simulated 2/3e events 97% were accepted with R < 40%, while 95% of the 1/3e events had R < 40%.

The computer also stored the pulse heights for each counter and printed them in the form of histograms, a feature which was particularly useful in calibrating the equipment.

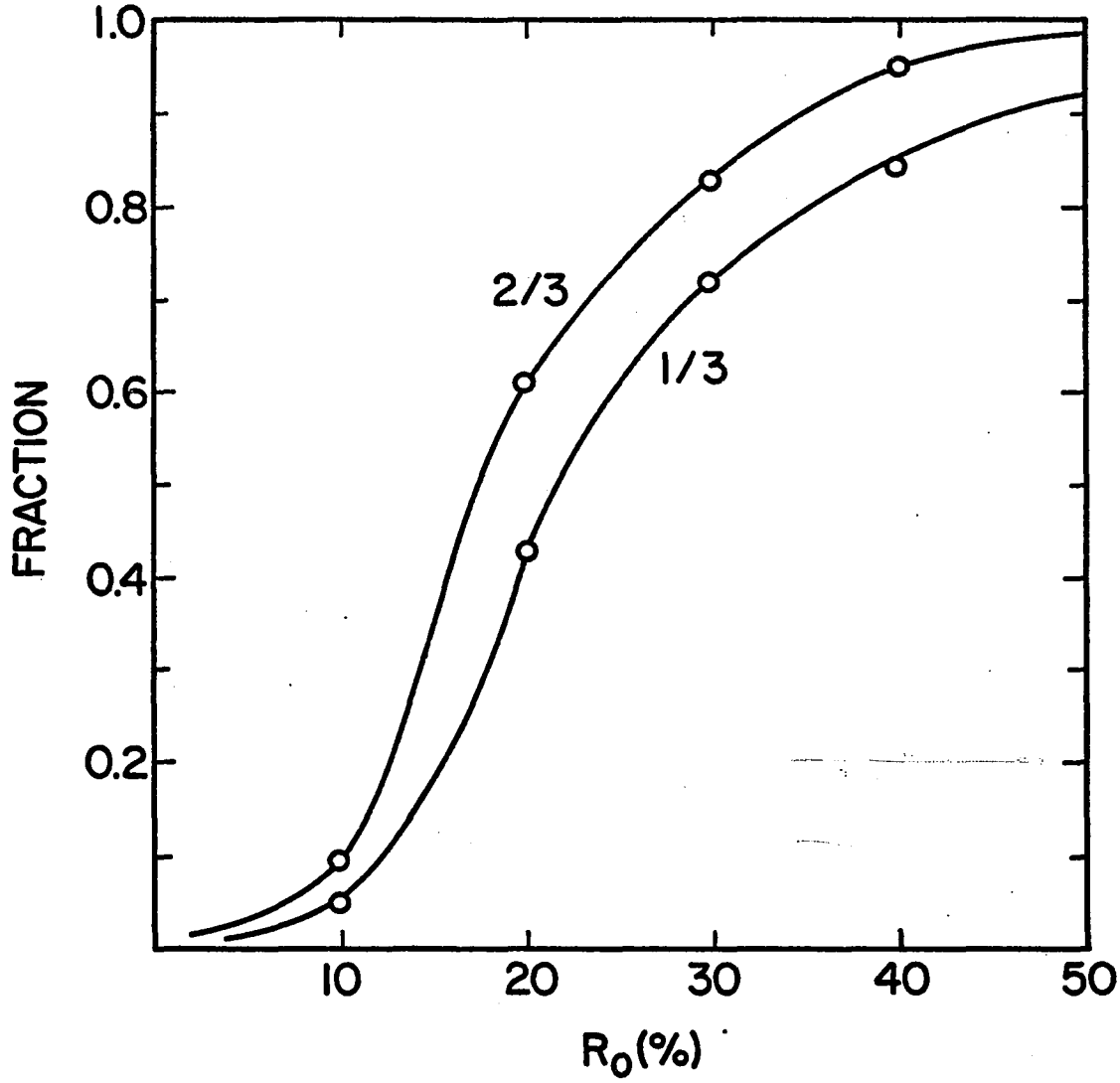

Figure 5 Fraction of the simulated quark events with R values less than a given percentage.

Calibration of the entire system was done after every 140 hours of continuous operation. A pulse height analysis was performed on the output of each of the 48 P.M. tubes using a multichannel analyzer. Their outputs were matched to a fixed standard from a tail pulse generator. All tube gains were adjusted to obtain agreement to within ± 5% of this standard. The efficiency of the system for accepting quarks was checked using the attenuating masks, and histograms of each counter's response to the simulated quark events and to unit charged particle events were obtained.

RESULTS

The equipment was operated for 1,504 hours, during which time functioning of the 2 sec. and 200 μsec. gates reduced the sensitive time to 1420 hours or 5.12×10^6 sec. Approximately 5.45×10^8 8-fold coincidences were examined by the logic circuits.

Roughly 60,000 events satisfied the quark-like pulse height requirements. That is, these events had pulse heights, I, in the range $0.04I_o < I < 0.76I_o$, where I_o is the most probable pulse height of a unit charged particle. Only events with values of R < 40% were recorded and analyzed by the computer, and there were 4,007 events of this type. Figure 6 shows the distribution of the average pulse heights, $\overline{P}_n$, of these events together with the same distribution for events with R < 30%, for comparison.

The spark chamber photographs of these events were analyzed for sparks defining an unaccompanied particle trajectory through the entire array. Events were accepted for further analysis which had a single track in at least one of the top two spark chambers that could be aligned with a single track in at least one of the bottom two chambers. Misalignment of tracks, extra tracks, or complete absence of a track in either pair was cause for rejection. Each event was examined independently two times. Any event

which had even a possibility of satisfying the above requirements was noted and very carefully examined a third time. One event survived the third examination.

The average pulse height for this event was 270 mV or $0.216I_0$, and the R value was 36.9%. Figure 6 shows the event relative to the background, while Figure 7 shows it relative to the two simulated quark distributions.

If the distributions of average pulse heights, $\overline{P}_n$, for simulated 1/3 and 2/3 quarks are normalized so they each have a total area of unity, they can be considered probability density functions, $f_{1/3}(x)$ and $f_{2/3}(x)$ respectively. For example, $f_{1/3}(x)dx$ represents the probability that a 1/3 quark event would have an average pulse height, $\overline{P}_n$, between x and x + dx, where x is measured in channels as in Figure 7. The probability that a 1/3 quark would produce an average pulse height of x_o or greater, $P_{1/3}(x \geq x_o)$, is given by the integral of $f_{1/3}(x)dx$:

$$P_{1/3}(x \geq x_o) = \int_{x_o}^{\infty} f_{1/3}(x)dx$$

When this integral is evaluated numerically for x_o equal to 270 mV (or channel 22), $P_{1/3}(x \geq x_o)$ is found to equal

$$P_{1/3}(x \geq x_o) = 0.004$$

In a similar way the probability that a 2/3 quark would produce an average pulse height as low or lower than x_o =

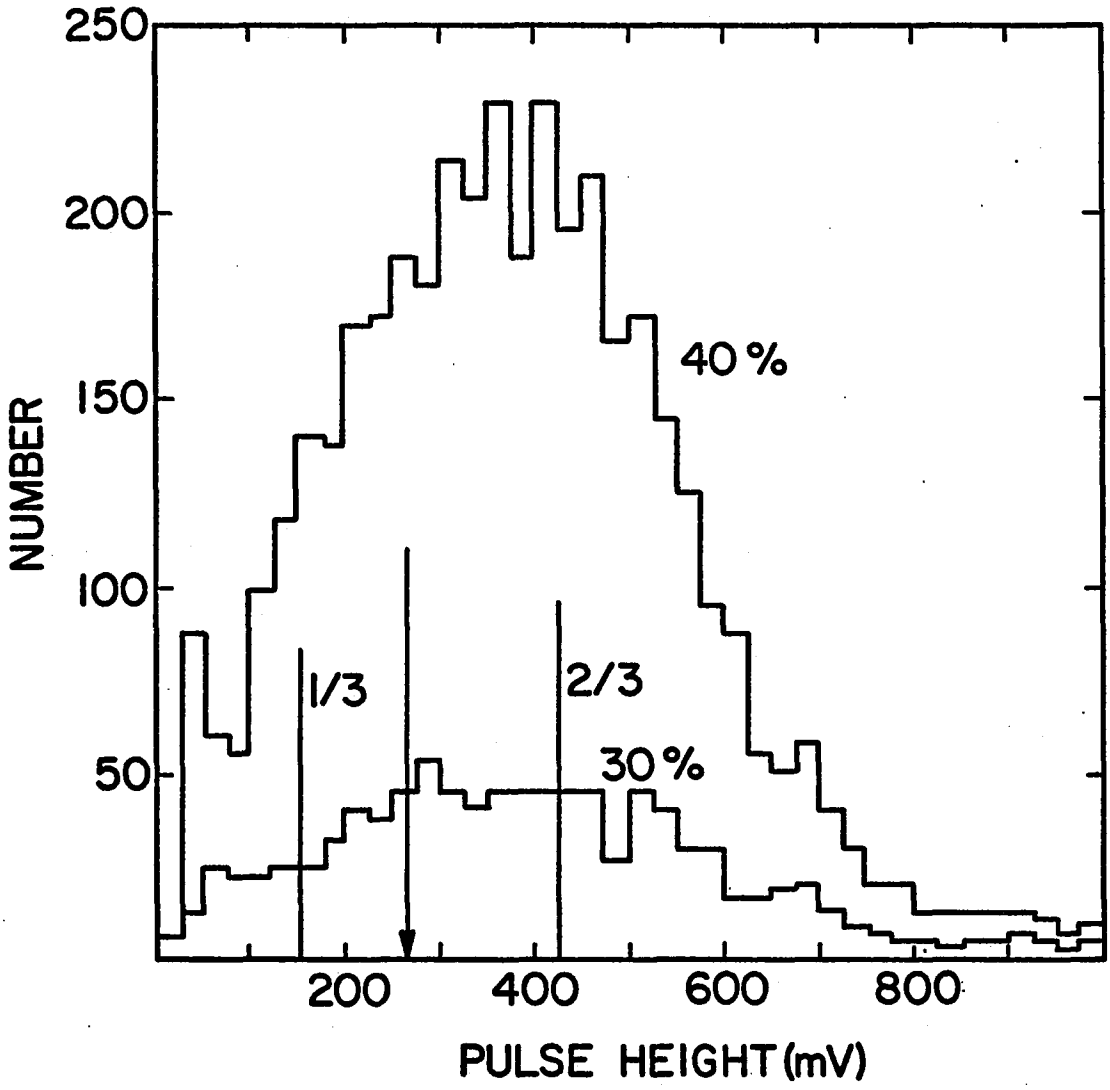

Figure 6 Background events at R<40% and R<30%. (Most probable simulated 1/3 and 2/3 quark pulse heights marked with vertical lines, one quark-like event pulse height marked by arrow.)

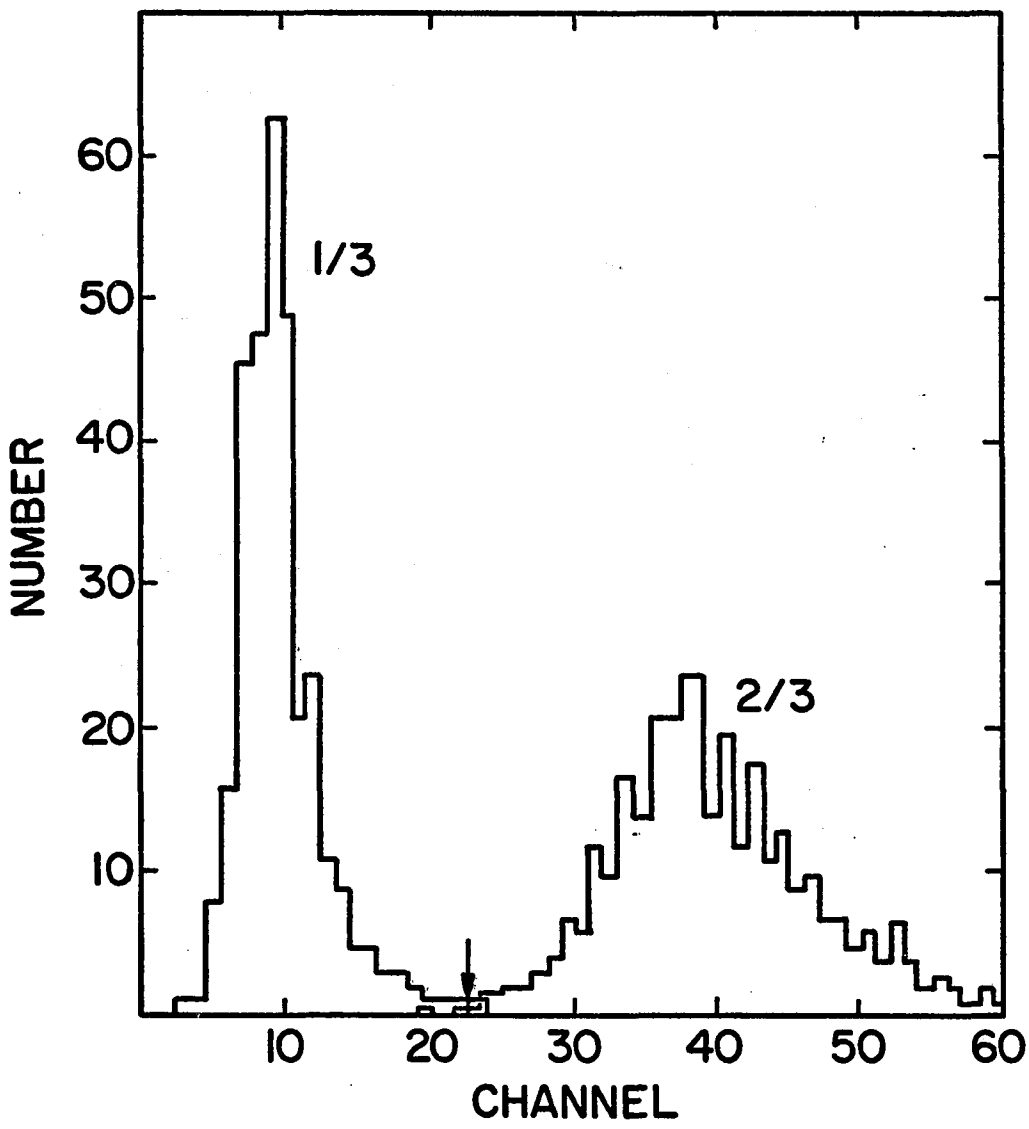

Figure 7 Simulated quark distributions showing pulse height of the one quark-like event (vertical arrow). (Each channel equals 12.2 mV)

270 mV would be found by integrating $f_{2/3}(x)$ from x_o to zero. $P_{2/3}(x \leq x_o)$ is found to be

$$P_{2/3}\ (x \leq x_o) = 0.008$$

These two probabilities are only approximate, due to the statistical nature of the histogram distributions used. However, they do give an indication of the likelihood that this pulse height (270 mV) was produced by either a 1/3 or a 2/3 quark.

The R value of this event, 36.9%, was quite high as compared to a typical simulated quark event. Figure 5 shows that only 18% of the simulated 1/3 quark events had R values equal to or greater than 36%, while only 12% of the simulated 2/3 quark events had R values this large. This event is, therefore, not considered to be a strong quark candidate; and in calculating the upper limits on quark fluxes, it was assumed that no quark-like events were observed.

DISCUSSION

Quark production by cosmic rays is expected to take place high in the atmosphere. The advantage of a mountain altitude quark search over a sea level experiment depends on the strength of the interaction of quarks with the atmosphere above the experimental site. If free quarks interact strongly with atmospheric nucleons and have an interaction mean free path short as compared to that for protons, very few might reach sea level detectors with relativistic velocities. The slower quarks would not be detected because of their increased ionization energy loss. If quarks are light particles with masses less than nucleon masses, again possibly few would be relativistic at sea level even if their mean free path is greater than that of protons.

Since most other cosmic ray quark searches have been done at sea level, it is convenient to "normalize" the results of a mountain altitude experiment to sea level. This allows a more direct comparison of experimental flux limits obtained by different experiments.

The counting rate, N, of a detector can be written in terms of the particle flux and the detector's geometry as follows:

$$N = \int_{\Omega} \int_{A} I \left| \cos \theta \right| d\Omega \, dA$$

where I is the quark flux (particles per unit area per unit solid angle per unit time), dA is an area element on the bottom counter, and $d\Omega$ is a solid angle element in the direction θ with the vertical looking through the top counter.

If the detector consists of an array of parallel plane counters, as in this experiment, then the counting rate is given by

$$N = \int_{A_1} \int_{A_2} I \, r_{12}^{-2} \cos^2 \theta \, dA_1 \, dA_2$$

where dA_1, dA_2, A_1, A_2, r_{12} and θ are illustrated in Figure 8. If the flux, I, is isotropic, it can be taken outside the integral, and N can be written as

$$N = I \int_{A_1 A_2} \int r_{12}^{-2} \cos^2 \theta \, dA_1 \, dA_2$$

or

$$N = I \, (A\Omega)_{\text{geometric}}$$

where

$$(A\Omega)_{\text{geometric}} = \int_{A_1 A_2} \int r_{12}^{-2} \cos^2 \theta \, dA_1 \, dA_2$$

The quantity $(A\Omega)_{\text{geometric}}$ is the geometric area solid angle product of a plane parallel detector array in an isotropic particle flux. It does not include weighting due to atmospheric absorption of either quarks or primary protons.

In order to include this absorption an "effective" area solid angle product can be defined (15). The counting

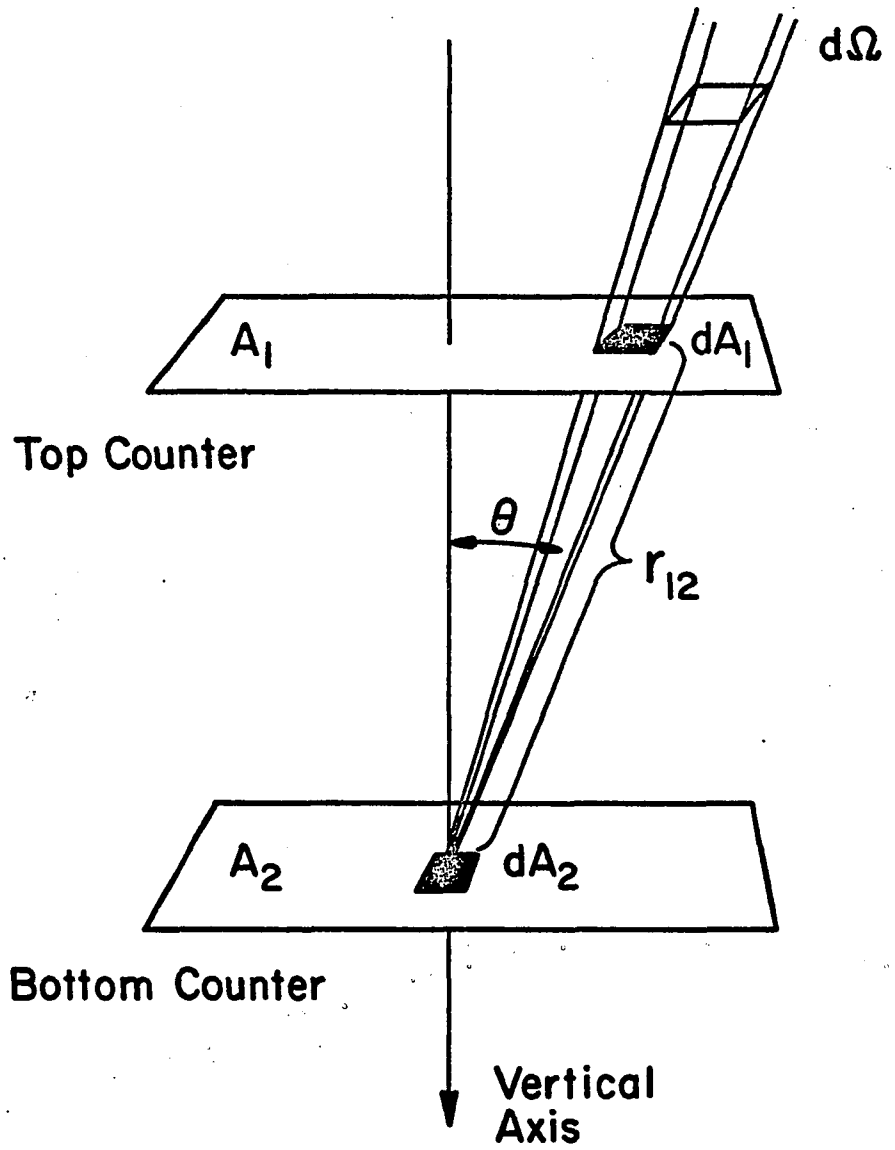

Figure 8 Counter geometry for AΩ calculation

rate can then be written as:

$$N(x) = I_q\left[\exp(\mu x_o)\int_{A_1}\int_{A_2} \exp(-\mu x \sec\theta) r_{12}^{-2} \cos^2\theta dA_1 dA_2\right]$$

where I_q is the vertical quark intensity at sea level, x_o is the atmospheric depth (gm/cm^2) at sea level, x is the atmospheric depth at mountain altitude and μ is the attenuation coefficient $\left[\mu = (\text{attenuation mean free path})^{-1}\right]$ for either primary protons or quarks, whichever is smaller. The quantity in brackets is the "effective" area solid angle product. With this definition an array with a given geometric area solid angle product becomes more "effective" for detecting quarks as it is brought from sea level to mountain altitude. The increase in effectiveness of an array thus depends on the size of the attenuation coefficient (or mean free path) used in the above equation. Note that if no attenuation is assumed, i.e., $\mu = 0$, the $(A\Omega)$ effective and $(A\Omega)$ geometric are identical.

An estimate of the inelastic interaction mean free path for quarks in the atmosphere can be calculated using the additivity principle of the quark model. The essence of this principle is that in high energy interactions between two hadrons (each of which is thought of as a cluster of quarks), the strength and character of the interaction results from the sum of the interactions of the individual quarks involved. At very high energy, exchange and

annihilation cross sections are expected to vanish and quark-quark scattering cross sections would equal quark-antiquark scattering cross sections. Under these conditions additivity can be used to estimate the ratios of various cross sections (28).

For example, from experimental data at high energy the ratio of the proton-proton scattering cross section to the pion-proton cross section is roughly 2/3 (28). From the additivity principle this seems reasonable, since the pion-proton interaction involves a quark-antiquark pair (the pion) incident on a proton target, while in the proton-proton interaction there are three quarks (the proton) incident.

When this argument is extended to the case of quark-proton scattering, the analogous ratio is

$$\frac{\sigma_{qp}}{\sigma_{pp}} \approx 1/3$$

where σ_{qp} is the quark-proton inelastic cross section, and σ_{pp} is the proton-proton inelastic cross section. Since atmospheric attenuation is being calculated, only the inelastic part of the total cross section is used. In the case of proton-proton scattering, the total cross section at high energy is about 40 mb. The inelastic part is about 30 mb. From the above ratio of σ_{qp} to σ_{pp} this would give an inelastic quark-proton cross section of about 10 mb at high energy.

The cross section for the interaction of a quark with the atmospheric nuclei (nitrogen is used for this calculation) is then estimated by the relationship

$$\sigma_{q\text{-nuclei}} = \pi\, r_n^2\, b$$

where r_n is the nuclear radius, and b is the nuclear opacity. The nuclear radius is calculated from the equation

$$r_n = 1.2\ A^{1/3} \times 10^{-15} \text{ meters}$$

where A is the nuclear mass number. Nuclear opacity is the probability that the quark will interact with a nucleon if it "strikes" the nucleus. Using the quark-proton cross section and integrating the interaction probability over the nuclear volume the opacity is found to equal 0.39. This finally leads to an inelastic interaction mean free path for quarks in the atmosphere of

$$\lambda_q = 226 \text{ gm/cm}^2$$

As a check, for protons in the atmosphere the inelastic interaction mean free path is calculated by the above method to be

$$\lambda_p = 120 \text{ gm/cm}^2$$

which is in reasonable agreement with measurements of absorption mean free path (11).

With these values for mean free path, flux limits can be calculated using the expressions for geometric or

effective AΩ. Three cases will be considered, and flux limits calculated. The first case involves no atmospheric attenuation, and (AΩ) geometric is used. In the second case quarks are assumed to be light particles ($M_q < M_p$) with the attenuation mean free path calculated above. The final case will allow quarks to be highly attenuated, with a mean free path shorter than that for protons. In this instance the proton attenuation coefficient, $\mu_p = 1/(120\ gm/cm^2)$, is used in the (AΩ) effective calculation.

In all three cases the counting rate, N, is of the form

$$N = \alpha\ I_q\ (A\Omega)$$

where AΩ is either the geometric or effective value, whichever is appropriate, α is the overall detector efficiency, and I_q is the quark flux. The upper limits on fluxes in the second and third cases, calculated using a value of (AΩ) effective, are thus "normalized" to values expected at sea level given the assumed conditions on absorption of quarks and primary protons.

With no quark events observed in 5.12×10^6 sec, the upper limit on N is $4.5 \times 10^{-7}\ sec^{-1}$ at the 90% confidence level. Table III gives the flux limits, together with AΩ values, for the three cases as well as the detector efficiencies.

Table III Area Solid Angle Products, Detector Efficiencies, and Flux Upper Limits

I Area Solid Angle Product

Case	AΩ(type)	Attenuation Coef. Used	AΩ
1	Geometric	$\mu = 0$	$0.627\ m^2 sr$
2	Effective	$\mu = 1/226\ gm/cm^2$	$1.982\ m^2 sr$
3	Effective	$\mu = 1/120\ gm/cm^2$	$5.51\ m^2 sr$

II Efficiencies

Spark Chamber Eff. = 93 %

±1/3e Quark Acceptance Eff. = 93 %

±2/3e Quark Acceptance Eff. = 80 %

III Upper Limit on Quark Flux*

Case 1: $I_q(\pm 1/3e) = 8.3 \times 10^{-11}\ cm^{-2} sr^{-1} sec^{-1}$
$I_q(\pm 2/3e) = 9.63 \times 10^{-11}\ cm^{-2} sr^{-1} sec^{-1}$

Case 2: $I_q(\pm 1/3e) = 2.62 \times 10^{-11}$
$I_q(\pm 2/3e) = 3.05 \times 10^{-11}$

Case 3: $I_q(\pm 1/3) = 0.945 \times 10^{-11}$
$I_q(\pm 2/3) = 1.09 \times 10^{-11}$

*at 90% confidence level

If quarks are produced with insufficient transverse momenta to carry them away from the other particles in the associated shower, they would escape detection in this experiment. The quark must be unaccompanied by other shower particles as it penetrates the counter array. If another particle, of unit charge, were coincident with a quark, the resulting signal would be roughly $(1 + 1/9)I_0$ or $(1 + 4/9)I_0$. In either case the signal would be lost in the unit charge distribution whose peak is I_0.

The probability that a vertically incident shower would have no particles hitting an array is given by the Poisson distribution

$$P(0) = \exp(-\Delta(r)\ A)$$

where $\Delta(r)$ is the density of shower particles (particles $/m^2$) incident on an array located a perpendicular distance, r, from the shower axis, and A is the area of the array in m^2. If it is required that this probability be 50% or greater, and A is $3.35m^2$, then the particle density cannot exceed $0.185m^{-2}$. If the array is sufficiently distant from the shower axis so that $\Delta(r)$ is less than $0.185m^{-2}$, then in 50% or more of the possible quark-producing interactions no shower particle would hit the array. A quark could then be detected with an efficiency greater than 0.5.

Assume a primary proton with energy, E_0, initiates a cosmic ray shower after penetrating into the atmosphere one inelastic interaction mean free path, 120 gm/cm. If

half of its energy goes into production of 10 secondary particles, and three of these are π^0's, then these π^0's would have energies of roughly $E_0/20$. They would quickly decay into two photons each, leaving a total of 6 photons with average energy $E_0/40$. The resulting electromagnetic cascade would produce an incident particle density, $\Delta(r)$, at a depth of 750 gm/cm^2 which can be calculated for various values of E_0 (29). This fixes the minimum distance from the shower axis at which a quark usually would be detected.

If quarks are produced symmetrically in the forward and backward directions in the proton-proton center of mass system, then half of the quarks would be found outside a cone of half angle θ in the laboratory system. This angle is given by

$$\tan \theta = (P_t/M_q)(2M_p/E_o)^{\frac{1}{2}}(1+(P_t/M_q)^2)^{-\frac{1}{2}}$$

where P_t is a quark's transverse momentum, M_q is the quark's mass, and M_p is the proton's mass.

Using the minimum radius from the shower axis of acceptably low shower density for a given E_0, and assuming that quark production takes place 12 km above the detector, a minimum value for tan θ can be calculated. Quarks produced outside the cone with half angle, θ, and penetrating a 3.35m^2 detector would be unaccompanied by unit charged particles at least 50% of the time. Such events would be observable in this experiment.

The minimum value of tan θ, $(\tan \theta)_{min.}$, at various primary proton energies defines a minimum transverse quark momentum, $(P_t)_{min.}$, for a given quark mass, M_q, above which at least half of the quarks would be detectable 50% of the time. The relationship is

$$(P_t)_{min.} = M_q(\tan \theta)_{min.}(2M_p/E_o - (\tan\theta)^2_{min.})^{-\frac{1}{2}}$$

Figure 9 shows the minimum values for P_t as a function of M_q for E_o equal to 10^{13} eV. The sensitivity of this experiment would rapidly become negligible as the quark transverse momentum decreases below $(P_t)_{min.}$, and would approach 100% as the transverse momentum increases above $(P_t)_{min.}$.

Figure 10 is a plot of the ratio $M_q/(P_t)_{min.}$ versus primary energy, E_o. A given primary interaction at energy, E_o, producing a quark of mass M_q with transverse momentum, P_t, can be represented by a point on the $M_q/(P_t)_{min.}$ versus E_o plane. If that point is located above the curve of Figure 10, then our experiment would have had low sensitivity to the quark produced. Conversely, our experiment would have been quite sensitive to quarks produced in interactions represented by points below the curve. A horizontal line drawn at the 10^{13} eV level intersects the curve of Figure 10 at a value of the ratio $M_q/(P_t)_{min.}$ equal to 69. This is the slope of the curve in Figure 9 which plots $(P_t)_{min.}$ vs M_q for E_o equal to 10^{13} eV. Similar curves can be obtained from Figure 10 for other primary energies.

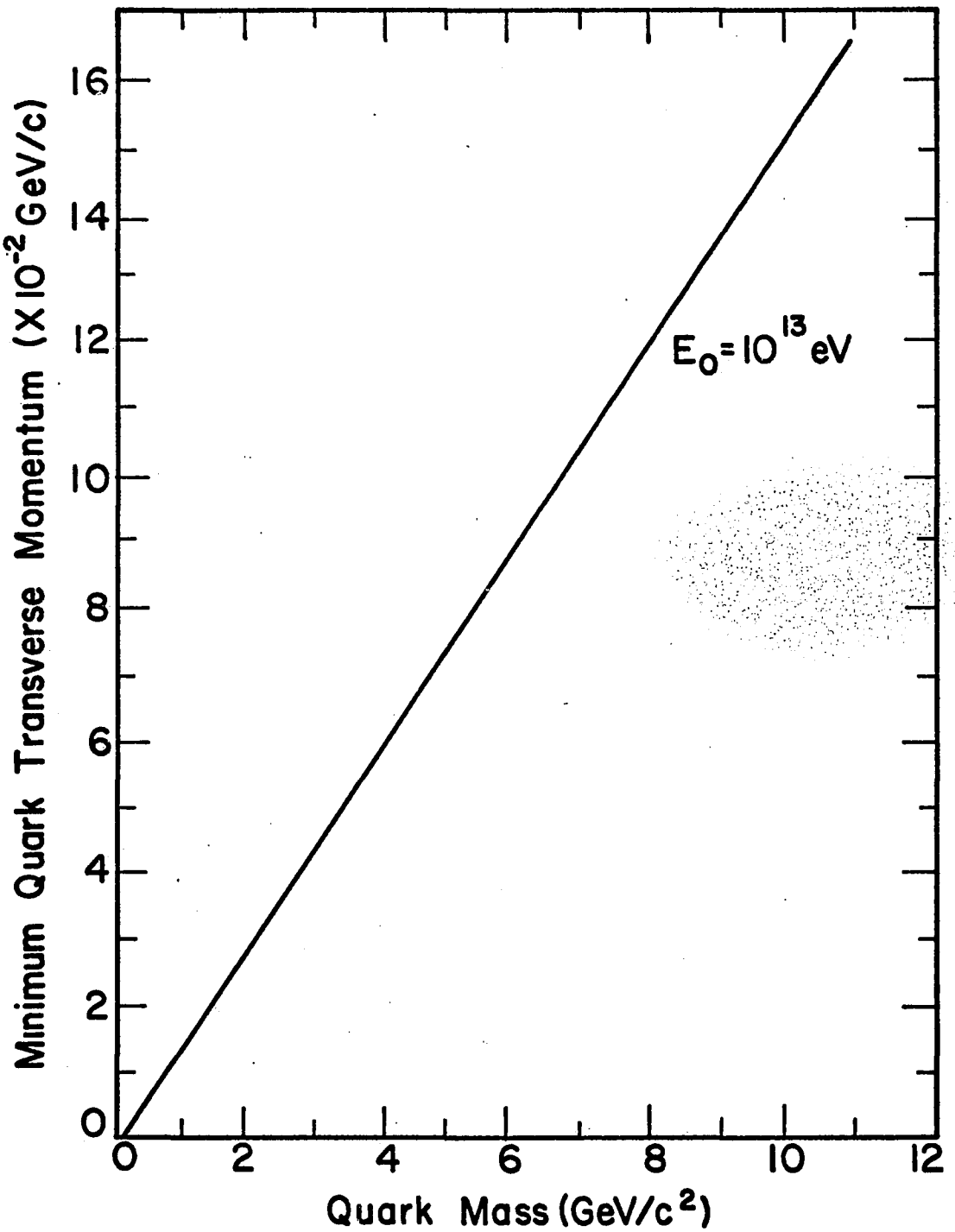

Figure 9 Minimum quark transverse momentum required so that half of the quarks produced would be detectable 50% of the time

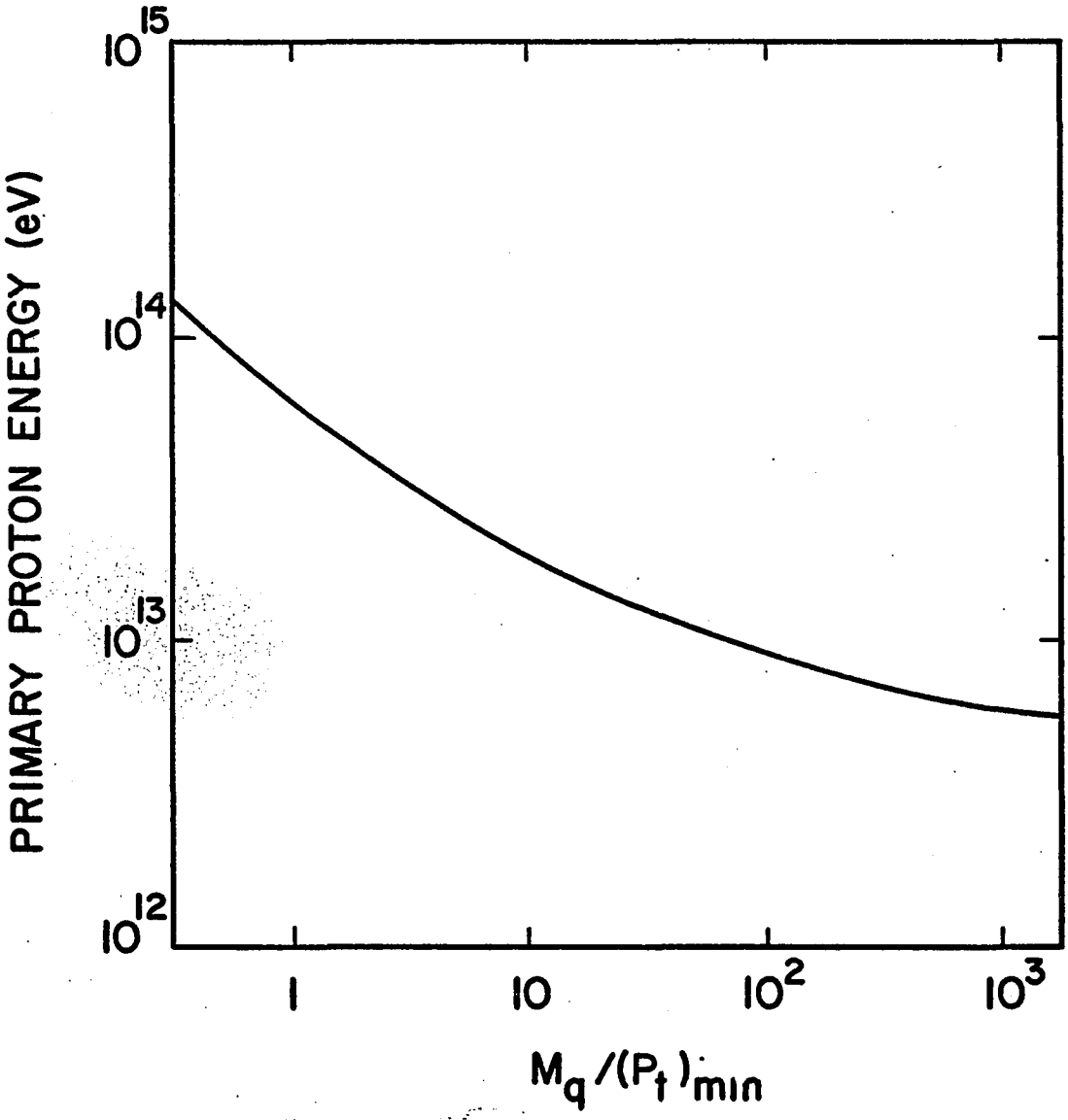

Figure 10 Sensitivity range of experiment
(Quarks produced in events represented by points below the curve could probably be detected)

At 10^{14} eV the ratio $M_q/(P_t)_{min.}$ is nearly zero, indicating $(P_t)_{min.}$ is very large for finite values of M_q. Our experiment had very low sensitivity to quarks produced at this energy or above. Such quarks would be quite rare, however, since the primary proton flux at energies greater than 10^{14} eV is of the order of 10^{-8} cm^{-2} sec^{-1} sr^{-1} (30). Even if the quark production efficiency were as high as 1%, and if there were no atmospheric absorption of quarks, an apparatus the size of ours would require considerably more than 1,500 hours to reliably detect such a low quark flux.

A comparison of the results of the McCusker group's experiment with this experiment is inconclusive. They observed four quark-like events in shower cores. In all four cases the "quark" tracks were accompanied by several hundred other shower particles per square meter. Our equipment is completely insensitive to such events. For one of the events, they estimate the "quark" to have been produced by the interaction of a 10^{15} eV primary proton, an energy beyond the sensitive region of our experiment.

The flux limits obtained at mountain altitude in this experiment are roughly the same as those obtained at sea level by other experiments. Within the energy and transverse momentum limits on sensitivity of this experiment the unweighted quark fluxes do not exceed the following limits at the 90% confidence level:

$$I_q(\pm\ 1/3e) < 8.3 \times 10^{-11}\ cm^{-2}\ sec^{-1}\ sr^{-1}$$

$$I_q(\pm\ 2/3e) < 9.6 \times 10^{-11}\ cm^{-2}\ sec^{-1}\ sr^{-1}$$

These limits are obtained by considering the quark to be massive ($M_q >> 1$ GeV/c^2) and unattenuated by the atmosphere ($\mu_q = 0$).

The flux of primary protons with energies above 10^{12} eV is 10^{-5} cm^{-2} sec^{-1} sr^{-1} (30). Assuming these protons are sufficiently energetic for quark production and that such production takes place in the first 120 gm/cm^2 of atmospheric penetration, the upper limits on quark production efficiency, ε, can be estimated. For unattenuated quarks, produced by primary protons with energies of 10^{12} eV or greater, the upper limits on production efficiency would be

$$\varepsilon\ (1/3) < 8.3 \times 10^{-6}$$

$$\varepsilon\ (2/3) < 9.6 \times 10^{-6}$$

at the 90% confidence level.

If quarks are light, with $M_q \simeq .4$ GeV/c^2 and are attenuated by the atmosphere with $\mu_q = 1/(226.\ gm/cm^2)$, then the flux limits normalized to sea level are

$$I_q(\pm 1/3e) < 2.6 \times 10^{-11}\ cm^{-2}\ sec^{-1}\ sr^{-1}$$

$$I_q(\pm 2/3e) < 3.1 \times 10^{-11}\ cm^{-2}\ sec^{-1}\ sr^{-1}$$

Under these conditions the production efficiency would have upper limits of

$$\varepsilon\ (1/3) < 1.4 \times 10^{-4}$$

$$\varepsilon\ (2/3) < 1.6 \times 10^{-4}$$

at the 90% confidence level. Absorption of quarks in the array would raise the flux and production limits by a factor of 1.7.

It hardly seems practical, by an extension of the same experimental technique to lower these limits by, say, an order of magnitude. This would require either increasing the $A\Omega$ of the array by a factor of 10 (physically difficult in the present laboratory) or increasing the running time to roughly 30 months (impractical, given graduate student temperament).

Quark searching will continue, however, as higher energy accelerators are completed. The colliding beam machine planned at CERN, is expected to provide proton-proton center of mass energies of 56 GeV, equivalent to a single beam laboratory energy of 1,700 GeV. The accelerator under construction at the National Accelerator Laboratory in Illinois is expected to reach laboratory energies of 400 GeV. Future quark searches are planned at both of these machines, and the beam intensities, as compared to primary cosmic ray intensities at these energies, should extend the data on quark production.

REFERENCES

1. Gell-Mann, M., Phys. Letters 8, 214 (1964).

2. Zweig, G., CERN Report 8419/TH, 412 (1964).

3. Lipkin, H. J., Phys. Rev. Letters 16, 1015 (1966).

4. Becchi, C., and G. Morpurgo, Phys. Rev. 140 No. 3B, B687 (1965).

5. Rubinstein, H. R., and F. Scheck, Phys. Rev. 154 No. 5, 1608 (1967).

6. Misra, S. P., and C. V. Sastry, Phys. Rev. 172 No. 5, 1402 (1968).

7. Dorfan, D. E., J. Eades, L. M. Lederman, W. Lee, and C. C. Ting, Phys. Rev. Letters 14, 999 (1965).

8. Blum, W., S. Brandt, V. T. Cocconi, O. Czyzewski, J. Danysz, M. Jobes, G. Kellner, D. Miller, D. R. O. Morrison, W. Neale, and J. G. Rushbrooke, Phys. Rev. Letters 13, 353 (1964).

9. Bellamy, E. H. R. Hofstadter, W. L. Lakin, M. L. Perl, and W. T. Toner, Phys. Rev. 166, 1391 (1968).

10. Antipov, Yu. M., I. I. Karpov, V. P. Khromov, L. G. Landsberg, V. G. Lapshin, A. A. Lebedev, A. G. Morosov, Yu. D. Prokoshkin, Yu. V. Rodnov, V. A. Rybakov, V. A. Rykalin, V. A. Senko, B. A. Utochkin, N. K. Vishnevsky, F. A. Yetch, and A. M. Zajtzev, Phys. Rev. Letters 29B, 245 (1969).

11. Jones, L. W., D. E. Lyon, Jr., P. V. R. Murthy, G. DeMeester, R. W. Hartung, S. Mikamo, D. D. Reeder, A. Subramanian, B. Cork, B. Dayton, A. Benvenuti, E. Marquit, P. D. Kearney, A. E. Bussian, F. Mills, C. Radmer, and W. R. Winter, Phys. Rev. 164, 1584 (1967).

12. Kasha, H., and R. J. Stefanski, Phys. Rev. 172, 1297 (1968).

13. Ashton, F., H. J. Edwards, and G. N. Kelly, Phys. Letters 29B, 249 (1969).

14. DeLise, D. A., and T. Bowen, Phys. Rev. 140, 458 (1965).

15. Krider, E. P., T. Bowen, and R. M. Kalbach, Phys. Rev. 1, 835 (1970).

16. McCusker, C. B. A., and I. Cairns, Phys. Rev. Letters 23, 659 (1969).

17. Cairns, I., C. B. A. McCusker, L. S. Peak, and R. L. S. Woolcott, Phys. Rev. 186 No. 5, 1394 (1969).

18. Adair, R. K., and H. Kasha, Phys. Rev. Letters 23, No. 23, 1355 (1969).

19. Frauenfelder, H., U. E. Kruse, and R. D. Sard, Phys. Rev. Letters 24 No. 1, 33 (1970).

20. Rahm, D. C., and R. I. Louttit, Phys. Rev. Letters, 24 No. 6, 279 (1970).

21. Chu, W. T., Y. S. Kim, W. J. Beam, N. Kwak, Phys. Rev. Letters 24 No. 16, 917 (1970).

22. Allison, W. W., M. Derrick, G. P. Hunt, J. D. Simpson, and L. Voyvodic, Phy. Rev. Letters 25 No. 8, 550 (1970).

23. Papastamatiou, N. J., Phys. Rev. 164 No. 5, 1784 (1967).

24. Schiff, L. I., Phys. Rev. Letters 17, 612 (1966).

25. Weyers, J., Phys. Rev. Letters 18, 1033 (1967).

26. Bowen, T., E. P. Krider, and J. W. York, Nuclear Instruments and Methods, 50, 349 (1967).

27. DeLise, D. A., and T. Bowen, Phys. Rev. 140, 458 (1965).

28. Kokkedee, J. J. J., and L. Van Hove, Nuovo Cimento 42, 711 (1966).

29. Cocconi, G., "Extensive Air Showers" Encyclopedia of Physics (Springer-Verlag, Berlin, 1961) Vol. XVI/1 pp 219-227.

30. Grigorov, N. L., A. U. Podgarskaya, L. V. Poperkava, Z. H. Sonelyeva, G. A. Skuridin, and A. F. Tikenkov, Proc. XI International Conf. on Cos. Rays. Budapest, CG-99 (1969).